RADIATION ONCOLOGY—ORIGINAL ARTICLE

Factors affecting target motion in stereotactic body radiotherapy of liver cancer using CyberKnife

Kevin MY Lo,[1] Vincent WC Wu,[2] Yu Li[3] and Hui Jun Xu[3]

1 Faculty of Health and Social Sciences, Hong Kong Polytechnic University, Kowloon, Hong Kong SAR
2 Department of Health Technology and Informatics, Hong Kong Polytechnic University, Kowloon, Hong Kong SAR
3 Department of Radiation Oncology, 302 Military Hospital, Beijing, China

KMY Lo DHSc; **VWC Wu** PhD; **Y Li** MD; **H Jun Xu** MD.

Correspondence
Dr Vincent WC Wu, Department of Health Technology and Informatics, Hong Kong Polytechnic University, Hung Hom, Kowloon, Hong Kong SAR.
Email: htvinwu@polyu.edu.hk

Conflict of interest: None.

Submitted 23 August 2019; accepted 12 February 2020.

doi:10.1111/1754-9485.13020

Abstract

Introduction: In stereotactic body radiation therapy (SBRT) of solitary liver cancer, organ motion due to respiration is an important factor in the definition of planning target volume (PTV). This study evaluated the potential associations of target motion with gross tumour volume (GTV) size, tumour location, Child–Pugh score and intra-fraction treatment time in SBRT of liver cancer treated by CyberKnife.
Methods: Translational motion data of 145 liver cancer patients, who were previously treated by CyberKnife with free breathing under tumour tracking, were recorded in the log files of the motion tracking system and analysed. The factors including target location based on liver segments, Child–Pugh score which was an indication of liver cirrhosis, GTV size and intra-fraction treatment time were recorded and their associations with the magnitude of target movement were evaluated.
Results: Target location demonstrated significant association with the translational target motion in the supero-inferior (SI) and left–right (LR) directions but less in antero-posterior (AP) direction. Tumours located at the peripheral segments were more affected than the central segments. Child–Pugh score and GTV size were not significantly associated with target motion in any direction. Longer intra-fraction treatment time generally increased target motion in the SI and LR directions.
Conclusion: In SBRT of liver cancer, the target motions in SI and LR directions were correlated with the location of target and treatment time, but not with Child–Pugh score and GTV size. These results should assist in deciding the GTV-PTV margin in SBRT treatment planning for solitary liver cancer.

Key words: liver cancer; stereotactic body radiation therapy; target motion; target location; GTV-PTV margin.

Introduction

Surgery has been the primary treatment modality for liver cancer. Due to the relatively high radiosensitivity of normal liver cells and the difficulty of preserving enough healthy liver tissues to avoid radiation-induced liver disease (RILD), conventional radiotherapy is usually not the treatment of choice. RILD is a serious radiation-induced complication with a mortality rate close to 80%.[1,2] Despite the liver being a parallel organ, the treatment of a small localized lesion is feasible if only a relatively small volume of normal liver cells is included in the target volume. The treatment of solitary liver lesions has been made possible with the introduction of stereotactic body radiation therapy (SBRT), which has emerged as a novel approach for delivering an ablative dose of radiation to liver lesions under a hypo-fractionated scheme. SBRT provides a highly conformal isodose distribution to the target with a steep dose fall-off and high precision treatment delivery.[3–5] As a result, improved tumour control[6,7] and reduced toxicity[8–10] in treating liver cancer using SBRT have been reported.

The liver poses a significant challenge for precision radiotherapy, due to movement from respiration and

Journal of Medical Imaging and Radiation Oncology

proximity to luminal structures with variable filling. Intra-fractional respiratory motion increases the uncertainty in target delineation and often increases the normal liver tissue irradiation. To better monitor the target dose due to respiratory motion and to reduce treatment uncertainty, different motion management methods have been used. They include gating, breath-holding or tracking, while some choose not to control the motion but instead deliver the radiation in a relatively short time or increase the margin for planning target volume (PTV).[11,12]

The healthy liver is a homogeneous soft tissue organ and consists of 8 segments according to the Couinaud classification (Fig. 1). Its motion during respiration is fairly uniform across the segments. However, 80%-90% of liver cancer patients have concurrent cirrhosis,[13] which may cause liver deformation and non-uniform motion among the different segments, that affects the mean tumour motion during respiration.[14,15] The degree of cirrhosis and liver stiffness is associated with the Child–Pugh score,[16] which is an indicator of the prognosis in liver cancer. Due to the steep dose gradients and relatively low number of fractions in SBRT, it is more sensitive to intra-fraction motion, which can potentially lead to significant errors in dose delivery up to as high as 20%.[17,18] Therefore an accurate estimate of liver motion is important in liver SBRT.

This study aimed to evaluate four variables which may affect the motion of the target tumour in liver cancer patients treated with SBRT using CyberKnife. Target motion was measured directly by monitoring the motion of implanted fiducials in two orthogonal X-ray images. The potential contributing factors were (i) tumour location (segment of liver), (ii) tumour size, (iii) the Child–Pugh score for chronic liver disease (an associated factor of liver condition and stiffness) and (iv) intra-fraction treatment time. The outcome of this research should help radiation oncologists to predict the extent of liver target motion and define an optimal margin for the PTV to avoid unnecessary irradiation of healthy liver tissue.

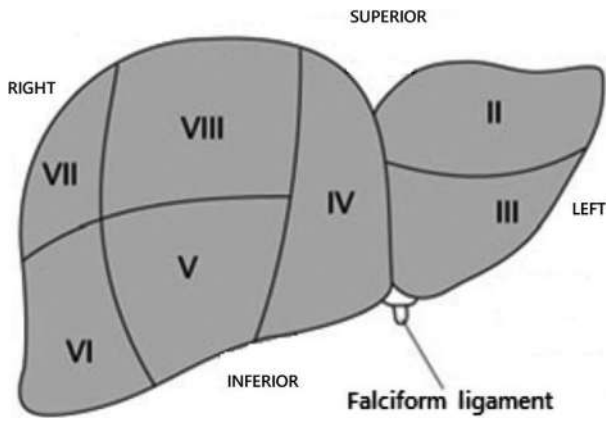

Fig. 1. Anterior view of the liver showing the anatomical location of various segments. Segment 1 is hidden behind segments 2 and 4.

Methods

The treatment histories of 146 patients with liver cancer from PLA301 Hospital in Beijing, China, were reviewed. The inclusion criteria were as follows: patients presented with unifocal liver lesion; with age greater than 18 years old; and treated with CyberKnife robotic radiosurgery system (Accuray Inc., Sunnyvale, CA, USA) between March 2014 and November 2015. All patients were treated under free breathing with basic body immobilization by BodyFIX Vacuum Cushions (Elekta AB, Stockholm, Sweden). Ethical approval was obtained from the hospital and the Hong Kong Polytechnic University. The patient identifiers were removed, and requirements of the Personal Data (Privacy) Ordinance were adhered to.

Child–Pugh score, which was categorized into class A, class B and class C, was recorded by the pathology department in the hospital prior to treatment. Three to eight gold fiducial markers (0.8 mm diameter $\times$ 5 mm long) were implanted into each patient around the target in a three-dimensional pattern (covering the *x*, *y* and *z* axes) for target tracking about one week before treatment. This allowed any potential fiducial migration to be completed during the first week, and the fiducials were expected to stay at the same position subsequently. All patients underwent four-dimensional (4D) CT scan with contrast. The exhaled-CT data set was used to delineate the GTV, from which the PTV was created by adding 2 mm margin for treatment planning. The delineation of GTV, PTV, organs at risk (OARs) and other structures were performed by the same group of radiation oncologists to avoid interpersonal variance using the Multiplan treatment planning system version 4.5.2 (Accuray Inc.).

In the treatment of the patients, all visible fiducial locations for each fraction were recorded by the Synchrony Respiratory Monitoring System of the CyberKnife unit in the respective log files, which were stored in the CyberKnife Target Location System (TLS) computer and collected for data analysis. This system was unique in CyberKnife which could perform near real-time monitoring of the movement of the target in the chest or abdomen, and apply corresponding corrections to the radiation beam when there was target movement due to respiration. The treatment time per fraction (in minutes) was obtained from the time recorded in the log file of each treatment.

The coordinates of the centroid of the GTV (target) for each treatment fraction were extracted from Synchrony log files and imported to Excel (Microsoft Excel for Mac 2011, version 14.3.9). The maximum target centroid displacements in left–right (LR) (X), supero-inferior (SI) (Y) and antero-posterior (AP) (Z) directions were recorded, which indicated the respective translational target displacements of the target in that specific fraction. In addition, the resultant three-dimensional (3D) displacement was calculated by taking the root mean square (RMS) of the three translational movements (X, Y and Z

directions). The average target displacement of each patient was obtained by averaging the translational centroid displacement data of all fractions.

Statistical analysis

The average target displacements in each translational direction were analysed by tumour location, tumour size (GTV), Child–Pugh class and intra-fraction treatment time. The average target displacements were first evaluated using the Shapiro–Wilk test for normally distributed data. Analysis of variance was used to compare tumour locations in eight liver segments. The continuous variables, GTV size and intra-fraction time, were analysed using linear regression. All patients were classified as having Child–Pugh class A or class B liver disease: class C patients were not treated with SBRT. Differences in average target displacements between the two Child–Pugh classes were tested using the Student *t*-test. All statistical analyses were done using SPSS (IBM, New York, NY, USA, SPSS statistics version 21).

Results

All patients were treated between 2 and 8 fractions with dose per fraction ranged from 4.5 Gy to 13.5 Gy (mean 8.13 Gy). All tumours showed movement during treatment with varying magnitude, with the supero-inferior (Y) direction motion being the largest and antero-posterior (Z) motion being the smallest among the three translational directions. All target displacement data were normally distributed after exclusion of one outlier who had an extremely high Y displacement. The patient characteristics and clinical information for the remaining 145 patients are summarized in Table 1. A summary of the translational movements of the tumour is shown in Table 2.

Table 1. Patient characteristics and clinical information (n = 145)

	No. of patients	%	
Gender			
Male	106	72.6	
Female	40	27.4	
Age (Years)			
Median			54.0
Range			36-82
GTV size (cm^3)			
Median			215.5
Range†			11.0-832.5
Maximum GTV diameter (cm)			
≤5	37	25.4	
<5 and < 10	65	44.5	
≥10	44	30.1	
Tumour location			
Segment 1	8	5.5	
Segment 2	22	15.1	
Segment 3	6	4.1	
Segment 4	29	19.9	
Segment 5	21	14.4	
Segment 6	24	16.4	
Segment 7	18	12.3	
Segment 8	18	12.3	
Child–Pugh Classification			
class A	128	87.7	
class B	18	12.3	
class C	0	0	
Number of SBRT fractions			
2	4	2.7	
3	3	2.1	
4	2	1.4	
5	52	35.6	
6	19	13.0	
7	63	43.2	
8	3	2.1	

†Range after excluding one outlier.

Table 2. Overall translational movements of the target in the three directions (n = 145)

Direction	Target movement (mm) Mean ± SD
X (Left–Right)	8.5 ± 3.1
Y (Supero-Inferior)	9.6 ± 3.9
Z (Antero-Posterior)	4.1 ± 2.1

Tumour location

Analysis of variance showed significant differences between liver segments with respect to average displacement in the left–right X (P = 0.021) and supero-inferior Y (P = 0.007) directions, but not in the antero-posterior Z direction (p = 0.398). A summary of the tumour movements with respect to the various segments of the liver is listed in Table 3. In the left–right (X) direction, tumours located at segments 3 and 6 demonstrated the largest mean motion of 10.0 mm, closely followed by segment 7 with a mean of 9.8 mm, while segment 2 had the smallest mean motion of 6.8 mm. In the supero-inferior (Y) direction, segment 7 had the largest mean motion of 12.1 mm, closely followed by segment 6 with 11.4 mm, while segment 2 had the smallest mean motion of 7.0 mm. Average displacements in the antero-posterior (Z) direction were smaller, ranging from 3.3 mm (segment 8) to 5.2 mm (segment 3). In addition, tumours in segment 7 demonstrated the largest 3D displacement of 16.3 mm, while tumours in segment 2 were the smallest. The tumour motions located at peripheral segments (6 and 7) were higher than those segments near the central part of the liver (2 and 4).

Tumour size

There was no significant relationship between GTV size and target displacement in any direction (P = 0.65,

Table 3. Translation target movement and three-dimensional (3D) displacements for tumour arising in various segments of the liver

Tumour Location (Segment no.)	No. of patients (n = 145)	X direction	Y direction	Z direction	3D Displacement (mm)
		Magnitude of target movement Mean ± SD (mm)			
1	8	9.4 ± 4.1	10.0 ± 4.5	3.7 ± 1.3	14.2
2	22	6.8 ± 2.4	7.0 ± 2.9	3.8 ± 1.2	10.4
3	6	10.0 ± 2.5	10.0 ± 2.4	5.2 ± 2.1	15.1
4	29	8.4 ± 2.9	8.2 ± 2.9	4.0 ± 1.9	12.4
5	21	8.1 ± 2.4	9.7 ± 3.4	4.0 ± 2.1	13.3
6	23	9.7 ± 3.7	11.0 ± 5.2	4.9 ± 2.5	15.8
7	18	9.8 ± 3.0	12.1 ± 4.5	4.8 ± 2.7	16.3
8	18	8.1 ± 2.1	9.9 ± 2.4	3.3 ± 1.9	13.2

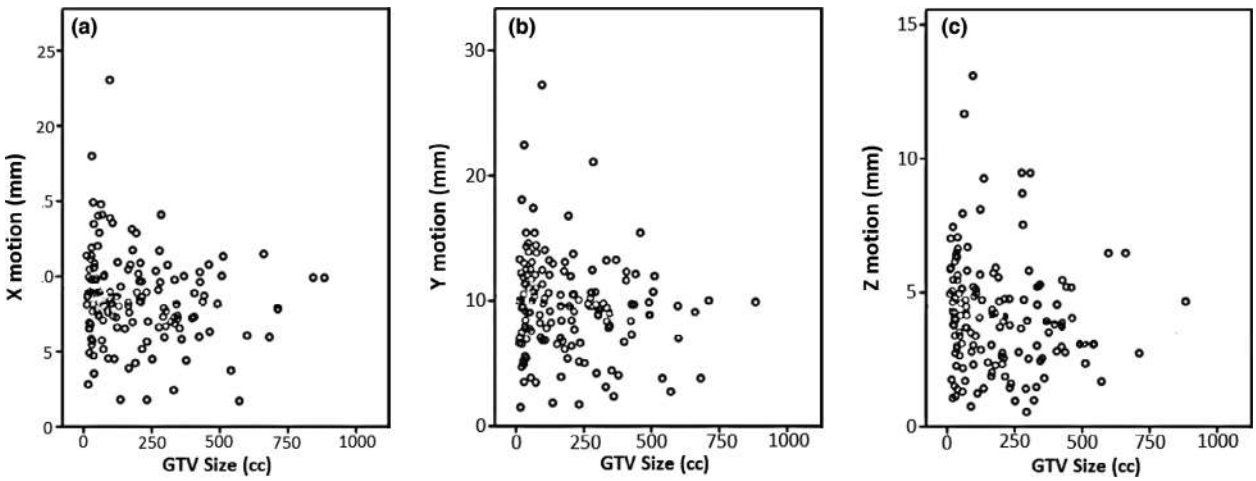

Fig. 2. Scatter plots showing the relationship between various translation motions with gross tumour volume size: (a) X (LR) direction, (b) Y (SI) direction and (c) Z (AP) direction (n = 144 after exclusion of two outliers).

0.59 and 0.71 for X, Y and Z directions, respectively) (Fig. 2a–c).

Child–Pugh class

The mean translation motions in all directions of the target were larger in patients with Child–Pugh class A than class B (Table 4).

Table 4. Translational motions of the target under different Child–Pugh classes

Child–Pugh Class	No. of patients (n = 145)	X direction	Y direction	Z direction
		Magnitude of target movement Mean ± SD (mm)		
A	127	8.8 ± 3.0	9.8 ± 3.9	4.2 ± 2.1
B	18	7.5 ± 3.1	8.3 ± 4.2	3.7 ± 2.4
	p (t-test)	0.092	0.13	0.35

However, the differences between classes were not statistically significant (P = 0.09, 0.13 and 0.35 for the X, Y and Z directions, respectively).

Intra-fraction treatment time

The mean treatment time was 46.1 ± 4.9 minutes, with a range of 36.3 to 61.5 minutes. There was a slight increase in displacement in the X (left–right) and Y (supero-inferior) directions with increasing intra-fraction time but no significant trends were observed for displacements in the Z direction (P = 0.032, 0.022 and 0.290 for X, Y and Z directions, respectively). The percentage of variances in target displacement accounted for by intra-fraction time (R^2) were 6.5%, 9.0% and 2.6% for X, Y and Z displacements, respectively (Fig. 3a–c).

Discussion

The magnitude of target motion in the liver was different among the three directions, with the SI (Y) direction

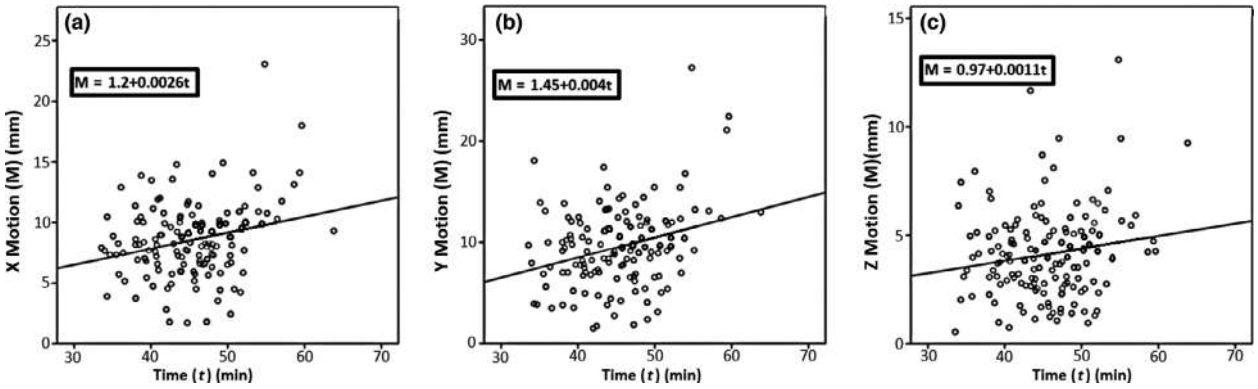

Fig. 3. Regression graphs showing the relationship between various translation motions (*M*) with treatment time (*t*) (n = 145). (a): X (LR) direction, (b): Y (SI) direction and (c): Z (AP) direction.

being the greatest and the AP (Z) direction the smallest. This is a common feature of the liver motion during respiration and has been reported in previous studies.[19,20] Since during respiration, the liver is largely affected by the diaphragm motion, which is mainly in the SI direction, the liver motion in this direction is the greatest. Moreover, according to Peeters et al.[21] during the later phase of inhalation, the inferior ribs move laterally and superiorly; this forces the liver to make a right side bending around an AP axis and move more medially. This explained the LR (X direction) motion of the liver during respiration.

In our study, the motion of the target in peripheral segments (6 and 7) was greater than that of the central segments (2 and 4). This was because during inhalation, the central tendon of the diaphragm descended less than the lateral parts.[21] In addition, the presence of coronary and falciform ligaments, which attach to the liver around the hilum of the liver from posterior and anchor it in the peritoneum, limited the motion of the liver around this region compared with the peripheral region. Based on these facts, it was logical to see that tumours located in different segments of the liver would experience different degrees of movement during respiration. For instance, tumours located in segment 7 demonstrated the greatest mean 3D displacement of 16.3 mm whereas those in segment 2 showed the least geometrical deviation. This also explained why there was a significant association of the target motion with the tumour locations.

With regard to the Child–Pugh scores, there was no patient belonging to class C in this study cohort. This was because class C referred to patients with poor liver condition and prognosis, and they were not suitable candidates for SBRT. There was no significant difference in target motion between the class A and class B patients in this study. A possible reason for this was because class A and class B patients have no or very mild cirrhosis and change of liver function; their impact on the liver motion was relatively small.

Despite the fact that hepatocellular tumours generally present with greater stiffness than normal liver parenchyma,[22] our results showed that there was no association between GTV size and the target motion. This implied that there was no significant influence of tumour stiffness on tumour motion. A possible reason for this was because the target motion was measured mainly based on the GTV centroid shift in this study. Since the centroid was the geometrical centre of the target, the effect of stiffness on the movement at this point might not be as great as at the target periphery, which would be more dependent on the target size.

Since a large dose per fraction is delivered in SBRT, it usually involves longer treatment time than conventional radiotherapy. The time is further increased in CyberKnife treatment due to its unique way of radiation delivery using robotic-controlled narrow beams. For instance, the mean treatment time obtained in this study was about 46 minutes which was longer than most linac-based SBRT. In our study, the mean translational movements in the three directions increased with treatment time. This could be explained by the fact that in the prolonged treatment time, the liver movement would be enhanced by internal organ motion and external body motion apart from the respiratory motion. Internal organ motion could be induced by the change of bowel and stomach conditions, whereas external body motion was induced by patient's own body movement due to the discomfort induced by long treatment time. Since the stomach and small bowel are situated medial and inferior to the liver, their changes in position would mainly affect the LR (X) and SI (Y) directions, respectively, and therefore relatively greater X and Y directional movements were observed. However, for the external body movement, it was expected to be random in nature and might not have a definite pattern.

Our results contribute information regarding the magnitude of the margin required when creating the PTV from GTV. First, we recommend a larger margin, for

instance at least 5 mm, for tumours located in the liver segments with greater movement (e.g. segments 6 and 7) compared to 2 mm for the segments with the smallest movement (e.g. segments 2 and 4). Different margins are recommended for the three directions in the body: wider margins are needed in the LR (X) and SI (Y) directions than in the AP (Z) direction. Margin modification for patients with large tumours or Child–Pugh score B liver disease is not required as we found no evidence that these factors affect target motion.

In conclusion, SBRT of liver cancer by CyberKnife, the target motions showed association with the tumour location mainly in SI and LR directions. Tumour situated in the peripheral segments tended to move more relative to the centrally situated segments. Target motion was also associated with the intra-fraction treatment time, but not with Child–Pugh score and GTV sizes. The results provided additional information for deciding the GTV-PTV margin.

Acknowledgements

The authors thank the Department of Radiation Oncology, 302 Military Hospital, Beijing, China.

References

1. Liang SX, Zhu XD, Lu HJ *et al*. Hypofractionated three-dimensional conformal radiation therapy for primary liver carcinoma. *Cancer* 2005; **103**: 2181–8.
2. Jun BG, Kim YD, Cheon GJ *et al*. Clinical significance of radiation-induced liver disease after stereotactic body radiation therapy for hepatocellular carcinoma. *Korean J Intern Med* 2018; **33**: 1093–102.
3. Soni PD, Palta M. Stereotactic body radiation therapy for hepatocellular carcinoma: current state and future opportunities. *Dig Dis Sci* 2019; **64**: 1008–15.
4. Chopra S, George K, Engineer R *et al*. Stereotactic body radio therapy for inoperable large hepatocellular cancers: results from a clinical audit. *Br J Radiol* 2019; **18**: 20181053.
5. Choi SH, Seong J. Stereotactic body radiotherapy: Does it have a role in management of hepatocellular carcinoma? *Yonsei Med J* 2018; **59**: 912–22.
6. Timmerman RD, Kavanagh BD, Cho LC, Papiez L, Xing L. Stereotactic body radiation therapy in multiple organ sites. *J Clin Oncol* 2007; **25**: 947–52.
7. Wigg AJ, Narayana SK, Le H *et al*. Stereotactic body radiation therapy for early hepatocellular carcinoma: a retrospective analysis of the South Australian experience. *ANZ J Surg* 2019; **89**: 1138–43.
8. Dawson LA, Hashem S, Bujold A. Stereotactic body radiation therapy for hepatocellular carcinoma. *Am Soc Clin Oncol Educ Book* 2012; 261–4.
9. Yeung R, Beaton L, Rackley T *et al*. Stereotactic body radiotherapy for small unresectable hepatocellular carcinomas. *Clin Oncol (R Coll Radiol)* 2019; **31**: 365–73.
10. Kim KH, Kim MS, Chang JS, Han KH, Kim DY, Seong J. Therapeutic benefit of radiotherapy in huge (>/=10 cm) unresectable hepatocellular carcinoma. *Liver Int* 2014; **34**: 784–94.
11. Gierga DP, Chen GT, Kung JH, Betke M, Lombardi J, Willett CG. Quantification of respiration-induced abdominal tumour motion and its impact on IMRT dose distributions. *Int J Radiat Oncol Biol Phys* 2004; **58**: 1584–95.
12. Campbell WG, Jones BL, Schefter T, Goodman KA, Miften M. An evaluation of motion mitigation techniques for pancreatic SBRT. *Radiother Oncol* 2017; **124**: 168–73.
13. Anaparthy R, Talwalkar JA, Yin M, Roberts LR, Fidler JL, Ehman RL. Liver stiffness measurement by magnetic resonance elastography is not associated with developing hepatocellular carcinoma in subjects with compensated cirrhosis. *Aliment Pharmacol Ther* 2011; **34**: 83–91.
14. Talwalkar JA, Yin M, Fidler JL, Sanderson SO, Kamath PS, Ehman RL. Magnetic resonance imaging of hepatic fibrosis: emerging clinical applications. *Hepatology* 2008; **47**: 332–42.
15. Wu H, Liang Y, Jiang X *et al*. Meta-analysis of intravoxel incoherent motion magnetic resonance imaging in differentiating focal lesions of the liver. *Medicine (Baltimore)* 2018; **97**: e12071.
16. Recio E, Macias J, Rivero-Juarez A *et al*. Liver stiffness correlates with Child-Pugh-Turcotte and MELD scores in HIV/hepatitis C virus-coinfected patients with cirrhosis. *Liver Int* 2012; **32**: 1031–32.
17. Wu QJ, Thongphiew D, Wang Z, Chankong V, Yin FF. The impact of respiratory motion and treatment technique on stereotactic body radiation therapy for liver cancer. *Med Phys* 2008; **35**: 1440–51.
18. Kawahara D, Ozawa S, Nakashima T *et al*. Interfractional diaphragm changes during breath-holding in stereotactic body radiotherapy for liver cancer. *Rep Pract Oncol Radiother* 2018; **23**: 84–90.
19. Kitamura K, Shirato H, Seppenwoolde Y *et al*. Tumour location, cirrhosis, and surgical history contribute to tumour movement in the liver, as measured during stereotactic irradiation using a real-time tumour-tracking radiotherapy system. *Int J Radiat Oncol Biol Phys* 2003; **56**: 221–8.
20. Liang Z, Liu H, Xue J *et al*. Evaluation of the intra- and interfractional tumour motion and variability by fiducial-based real-time tracking in liver stereotactic body radiation therapy. *J Appl Clin Med Phys* 2018; **19**: 94–100.
21. Peeters L, Lason G. The Liver and the Gallbladder Osteopathic Medicine, Chapter 3 Mobility P.24. The International Academy of Osteopathy; 2013.
22. Venkatesh SK, Yin M, Glockner JF *et al*. MR elastography of liver tumours: preliminary results. *AJR* 2008; **190**: 1534–40.